

# **Blast Analysis of Concrete Structural Elements Considering Material Strain Rate Effects**

Nikhil Dipak Kulkarni

A Dissertation Submitted to  
Indian Institute of Technology Hyderabad  
In Partial Fulfillment of the Requirements for  
The Degree of Master of Technology



भारतीय प्रौद्योगिकी संस्थान हैदराबाद  
Indian Institute of Technology Hyderabad

Department of Civil Engineering

July, 2013

## Declaration

I declare that this written submission represents my ideas in my own words, and where others' ideas or words have been included, I have adequately cited and referenced the original sources. I also declare that I have adhered to all principles of academic honesty and integrity and have not misrepresented or fabricated or falsified any idea/data/fact/source in my submission. I understand that any violation of the above will be a cause for disciplinary action by the Institute and can also evoke penal action from the sources that have thus not been properly cited, or from whom proper permission has not been taken when needed.

*Nikhil Dipak Kulkarni*

-----  
(Signature)

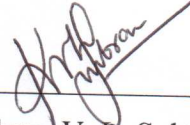
*Nikhil Dipak Kulkarni*

-----  
(Nikhil Dipak Kulkarni)

-----  
(Roll No: CE11M05)

## Approval Sheet

This thesis entitled Blast Analysis of Concrete Structural Elements Considering Material Strain Rate Effects by Nikhil Dipak Kulkarni is approved for the degree of Master of Technology from IIT Hyderabad.



---

Prof. Kolluru. V. L. Subramaniam  
Advisor and Examiner



---

Dr. Suriya Prakash  
Examiner

---

Dr. Ashok Kumar Pandey  
Examiner

## Acknowledgements

First and foremost I offer my sincerest gratitude to my guide and supervisor, Prof. K.V.L. Subhramaniam, who has supported me throughout my thesis with his patience, motivation and knowledge whilst allowing me the room to work in my own way. I attribute the level of my Master's degree to his encouragement and effort and without him this thesis, too, would not have been completed or written. One simply could not wish for a better or friendlier supervisor. Next I would like to thank Dr. Suriya Prakash and Dr. Ashok Pandey for showing their interest in evaluating my research work.

I would like to thank my parents for their encouragement, patience and support emotionally and otherwise. I would also like to thank Mr. Ravindra Gouda from Xitadel, for his support on LS-DYNA and resolving all the software related problems. I thank all my well-wishers for their blessings.

## Abstract

There has been an increased interest in the scientific and engineering communities, in recent times, towards developing understanding the blast response of structures and/or buildings. Blast produces transient loading of very short duration on a structural element. There are several time-scales in the blast response of the structural element. In the very short time scale (on the order of duration of the compression wave), the transient response is governed by the stress changes produced by wave propagation in the material. With time, the response of the structure evolves to produce vibration of the entire structural element at frequencies, which are determined by the stiffness of the element and the boundary conditions. The vibration response of the structural elements usually occurs in the millisecond time-scale. The vibration response might be completely absent in the case where complete failure or loss of integrity is the high amplitude stress wave produced by shock front. In the short time scales, a large magnitude blast can result in significant damage and even brittle shattering in concrete or masonry leading to a collapse of the structural element. The failure of a few critical load-bearing structural elements may eventually lead to the progressive collapse of the entire structure.

The effect of strain rate on the dynamic response of concrete is numerically investigated using the finite element software, LS-DYNA. This research primarily focusses on understanding the effects produced due to high strain rate loading on concrete, namely inertial confinement effect and the strain rate effect. At high strain rates failure is localized. When the strain rate is increased, localized failure is associated with the compressive stress wave generated in the material which produces an abrupt rise in the stress. The initial response is dictated by propagation of the stress wave in the material. The stress changes produced by the propagation of the stress wave are due to linear elastic wave for low strain rates. High strain rates are associated with stress changes produced by a non-linear compression stress wave. The passage of the wave produces irreversible damage and plastic deformation. At very high strain rates, a compression front which produces localized failure is transmitted in the material. The passage of the stress front produces complete crushing failure in the material. As the crushing front propagates in the material, the energy dissipation produced by the irreversible compaction of material produces an attenuation in the

stress amplitude. The magnitude of the stress achieved depends on the rate of loading and the inertial confinement effects. Both effects are important in determining the load response of a reinforced concrete structure. Confinement effects result in an increase in the stress magnitude for a given strain rate.

# Contents

.....	CHAPTER 1: Introduction	
.....		1
.....	CHAPTER 2: Literature Review	
.....		3
<b>2.1</b>	<b>Introduction</b> .....	3
<b>2.2</b>	<b>Strain rates and its effects</b> .....	3
<b>2.3</b>	<b>Rate of Damage</b> .....	8
<b>2.4</b>	<b>Confinement Effect</b> .....	9
.....	CHAPTER 3: Evaluation of Dynamic Response in Concrete.	
.....		11
<b>3.1</b>	<b>Introduction</b> .....	11
<b>3.2</b>	<b>Background</b> .....	12
<b>3.4</b>	<b>Results of Numerical Analysis</b> .....	17
<b>3.5</b>	<b>Material strain rate effect (Material response)</b> .....	23
<b>3.6</b>	<b>Evaluation of Confinement Effect</b> .....	27
.....	CHAPTER 4: Summary and Future Work	
.....		31
<b>4.1</b>	<b>Summary</b> .....	31
<b>4.2</b>	<b>Future work</b> .....	32
.....	References	
.....		33

## Figures:

Figure 1-1: The spherical propagation of blast waves. (FEMA428, December 2003)	1
Figure 2-2: Blast wave pressure – Time history (TM 5-1300, 1990)	1
Figure 2-1: Effect of Strain Rate on Compressive Strength (Bischoff, 1991)	5
Figure 2-2: Normalized concrete compressive strength vs. strain rate. (Yong Lu, 2004)	6
Figure 2-3: Effect of Strain Rate on Yield Stress of Steel Reinforcement (Malvar L. J., 1998)	6
Figure 2-4: Effect of Strain Rate on Tensile (Ultimate) Strength of Steel Reinforcement (Malvar L. J., 1998)	6
Figure 2-5: Normalized dynamic concrete tensile strength vs. strain rate. (Yong Lu, 2004)	7
Figure 2-6: The Stefan Effect. (Li & Zheng, 2004)	9
Figure 2-7: Stress-strain curves of concrete at different strain rates (Ngo, 2004)	9
Figure 3-1: Specimen sizes used in the numerical study	15
Figure 3-2: Boundary and loading conditions	16
Figure 3-3: Influence of Mesh size on the predicted response at 0.0125/s	19
Figure 3-4: Influence of Mesh size on the predicted response at 1/s	19
Figure 3-5: Influence of Mesh size on the predicted response at 10/s	20
Figure 3-6: Influence of Mesh size on the predicted response at 100/s	20
Figure 3-7: Comparison of material models for various strain rates	21
Figure 3-8: Comparison of inclusion and exclusion of rate effects for various strain rates in CSCM model	22



Figure 3-9: Comparison of inclusion and exclusion of rate effects for various strain rates in 72R3 model.....	23
Figure 3-10: The position of load histories plot on the columns.....	24
Figure 3-11: Comparison of stress histories predicted by 72R3 model for various strain rates. ....	26
Figure 3-12: Comparison of stress histories predicted by CSCM model for various strain rates. ....	26
Figure 3-13: A close up graph of the stress built up in both the material model at strain rate of 1/s. Note the time step of the peaks.....	27
Figure 3-14: The section at which stress histories along the diameter are plotted in the 4in × 32in and 16in × 32in columns. ....	28
Figure 3-15: Stress history along diameter for 4 × 32 inches 72R3 column at 5 in from top for various strain rates at various times. ....	29
Figure 3-16: Stress history along diameter for 16 × 32 inches 72R3 column at 5 inch from top for various strain rates at various times.....	29

# CHAPTER 1: Introduction

Blast is case of extreme loading. Blast waves propagate in the atmosphere through hemispherical (ground) or spherical (at some height from ground). The hemispherical propagation is a characteristic of the blast wave. Blast loading is a pressure loading or a stress loading on the structure. The applied pressure rises instantaneously and decays rapidly. The entire loading lasts for a few milliseconds. Idealized pressure time history: Except for very close-in blasts, a general time history as shown in following Figure 2-2 is applicable for nearly all blast loadings. Blast load produce out of plane loads on the structural members it encounters in its path. The influence of blast loading is localized, producing localized failure of elements. Localized failure of elements lead to a failure of the structure associated with progressive collapse.

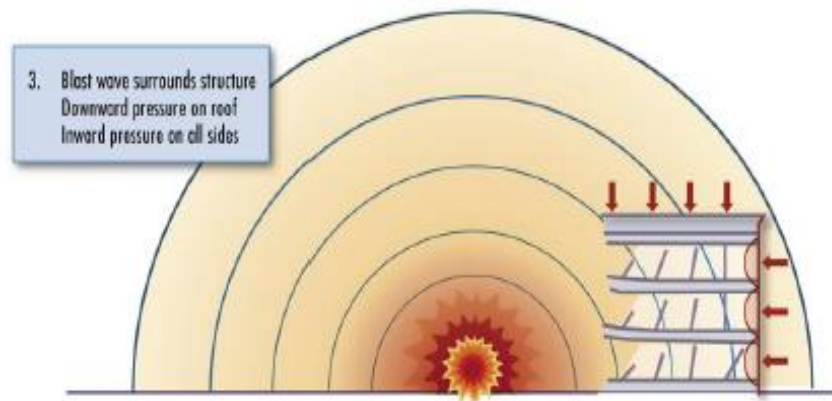


Figure 1-1: The spherical propagation of blast waves. (FEMA428, December 2003)

*Characteristics of blast pressure profile.*

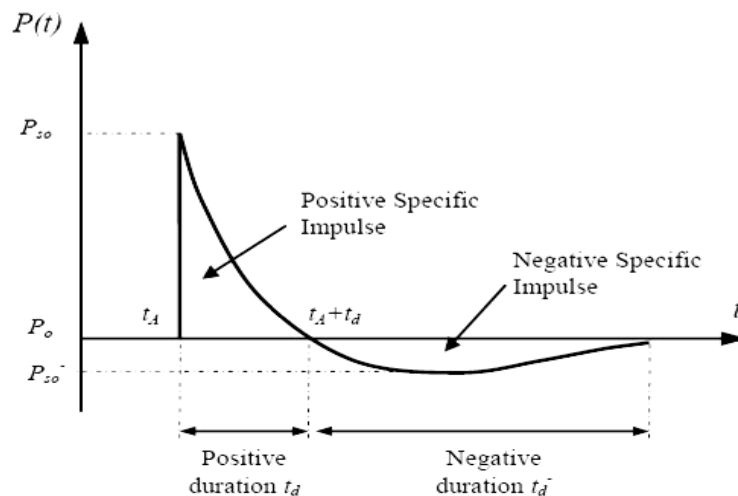


Figure 2-2: Blast wave pressure – Time history (TM 5-1300, 1990)

Most materials exhibit a strain rate dependent behavior, which have provision for increases in the elastic modulus and strength with an increase in the strain rate. In concrete structures, strength enhancement at high rates of loading originates from two phenomena: strain rate and lateral inertia confinement which latter is a function of the size of structure. The effect of strain rate can be controlled through a parameter included in the material models; however, the effect of the size of the structure on the strength enhancement cannot be controlled directly. In real structures, the effect of structure size on the strength enhancement can be significant.

LS-DYNA, is a finite element program capable of performing non-linear dynamic analysis, has several material models for concrete that were developed by researchers for different applications. This software program is used extensively in research projects to simulate the blast loading of structures and the structural response. LS-DYNA has several constitutive models to represent concrete. Choosing the material model that generate the closest numerical results in respect to experimental results or calibrating material models requires an understanding of the response of these concrete material models when subjected to high strain rates.

In this study high rates of loading associated with impact and blast, which affect the non-linear response of reinforced concrete structures, are evaluated. The effect of strain rate and the size of structure on the strength enhancement of three material models within LS-DYNA that are widely used to model concrete are investigated. The mesh size affects the accuracy of the results obtained from a finite element analysis. In this study the mesh sensitivity of three concrete material models of LS-DYNA subjected to three ranges of strain rate is investigated.

## **Organization of thesis**

This thesis is organized in four chapters. Chapter 2 contains the literature review where the basic concepts of blast are viewed. Chapter 3 contains the results from the numerical simulations and discussion over the results. It covers extensively the effect of strain rates and confinement. Chapter 4 talks about the summary, recommendations and future work.

# CHAPTER 2: Literature Review

## 2.1 Introduction

During an impulse loading, like explosion or an impact, structural materials experience a very high pressure shock wave in a very short period of time. Such loadings are termed as impact loadings. This type of loading subjects the structural material to very high strain rates. Hence it is necessary to understand effect of high strain rates on the behaviour of the materials.

Research on structural response for very high strain rates is limited and results are often not widely disseminated. There are many available tools (in terms of softwares) that are sophisticated, are available that make it possible to analyse with precision that exceed general understanding of structural response. Hence, a simplified approach of SDOF is basis for many designs. This approach is usually consistent with precision with which blast environment is modelled, and the knowledge of element behaviour and gives us an approximate level of damage in the material. While considering the elements as component of structural system under influence of blast loading, the response from a single element (or an individual element) can differ significantly from the global response.

## 2.2 Strain rates and its effects

The stress strain relationship for concrete is a function of strain rate (Bischoff, 1991), (Ross, 1995), (Malvar L. J., 1998) (Ross, 1995), (Hentz, 2004), (Schuler H, 2003.), and (Y. Hao, 2007) have reported on effect of strain rate on either compressive or tensile strength. The rate of loading vary from very low rates to high rates of strain. . The strain rate for structures subjected to creep is about  $10^{-7} \text{ s}^{-1}$ . For quasi-static loading, the strain rate is approximately  $10^{-5} \text{ s}^{-1}$ . During an earthquake, structures can be subjected to maximum rate of  $10^{-2} \text{ s}^{-1}$ . However, impact and blast loads subject structures to significant loads applied at a very short period of time which produces strain rates between 1 and  $1000 \text{ s}^{-1}$  (Bischoff, 1991). (Hentz, 2004)also presents the following ranges of strain rates for different types of loading:  $10^{-8}$  to  $10^{-7} \text{ s}^{-1}$  for creep,  $10^{-6}$  to  $10^{-5} \text{ s}^{-1}$  for quasi-static loading,  $10^{-4}$  to  $10^{-1} \text{ s}^{-1}$  for vehicle and plane impact, 10 to  $10^2 \text{ s}^{-1}$  for missile impact,  $10^{-4}$  to  $10^1 \text{ s}^{-1}$  for earthquake and induced shocks, and  $10^2$  to  $10^3 \text{ s}^{-1}$  and higher for blast loading (Hentz, 2004). The rate of loading has a significant influence on the response of visco-plastic structural materials including concrete. High

rates of loading affect material properties including compressive and tensile strength, modulus of elasticity, ductility, and Poisson's ratio (Bischoff, 1991).

Amongst the common beliefs, one that is widely accepted is that crack propagation in concrete occurs at a limiting velocity. Hence, the concrete cannot crack (or fail) quickly enough to keep up with a high rate of loading (Tedesco J. W., 1990). Another widely accepted theory is that concrete as a material itself is not strain rate dependent. Rather, it perceives an increased strength due to inertial confinement and the fact that concrete is pressure sensitive (as proposed by Stevens, 2009). Inertial confinement occurs when the material around the structural member or a part of a structural member cannot deform fast enough to respond with the member. Hence that member (or part of it) experiences existence of additional confinement generated by rigidly responding surrounding material. Regardless, concrete does have a strain rate threshold beyond which its strength increases significantly. The strain rate threshold for concrete response in tension is approximately  $2.5 \text{ s}^{-1}$ , and the strain rate threshold for concrete in compression is approximately  $30 \text{ s}^{-1}$ . The increase in strength can be calculated using Dynamic Increase Factors or DIFs. They are used for design purposes.

The rate effect has direct implications on the dynamic strength of concrete. For lower strain rates (typically below 30/s), there is not much effect on the dynamic strength of concrete. For high strain rates (more than 30/s) we do see a significant increase in the strength of concrete (Bischoff, 1991). The following graph describes the increase in the strength of concrete at high strain rates. The rate of loading affects the response of concrete to dynamic loading. As concrete is a heterogeneous material with inherent microcracks, discontinuities and voids that are initially present in the material, its behavior during static uniaxial loading is affected by the propagation of internal microcracks, which are tensile in nature and primarily oriented in the axial direction. During rapid loading, the time available for microcrack development or propagation is reduced. Hence, the strain rate dependent behavior of microcracking can influence the response when concrete is subjected to the very high rates of loading that occur during impact and blast. (Yong Lu, 2004).

Just like compression, the tensile strength of concrete increases with increase in rate of loading. Figure 2-4 represents the (normalized) increase in the tensile strength in high strain-rate regime for concrete. For both tension and compression, we can see

that concrete displays an exponential trend for relative increase in strengths. The trend is identical though the values differ, as it can be seen in figures 2-2 and 2-5.

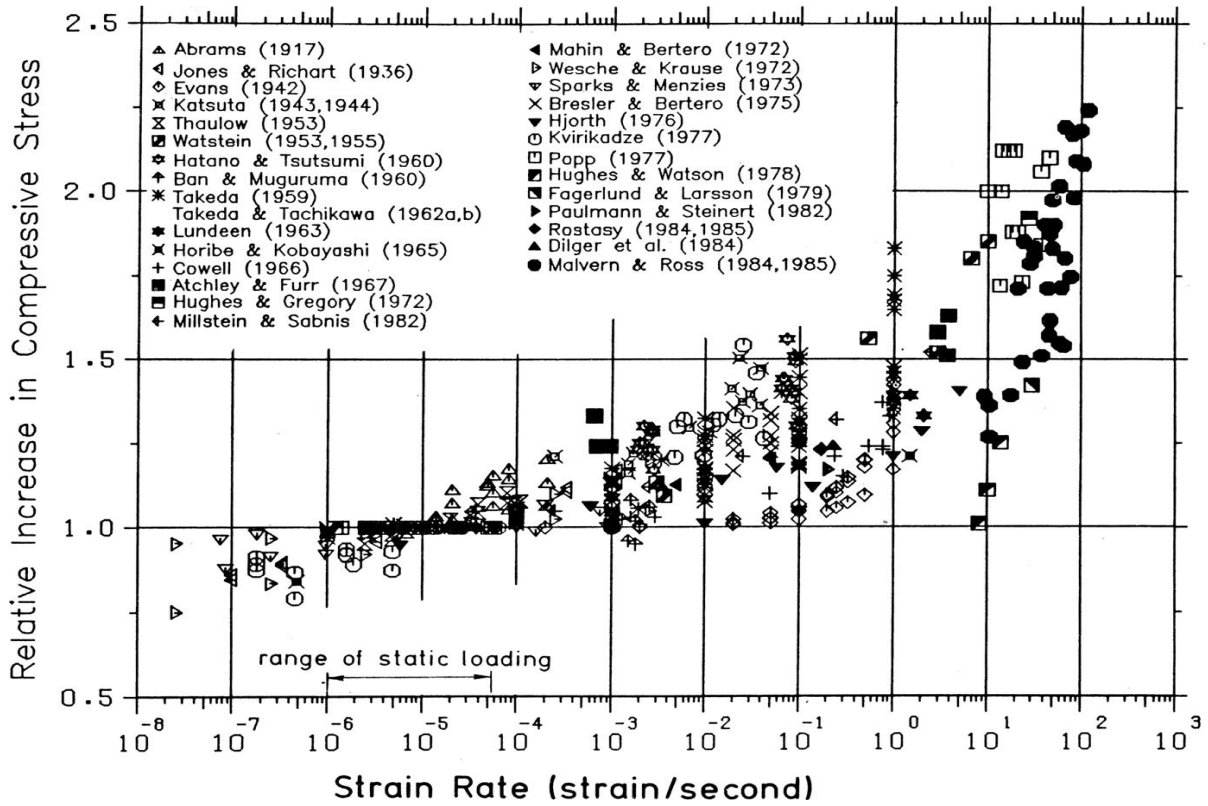


Figure 2-1: Effect of Strain Rate on Compressive Strength (Bischoff, 1991)

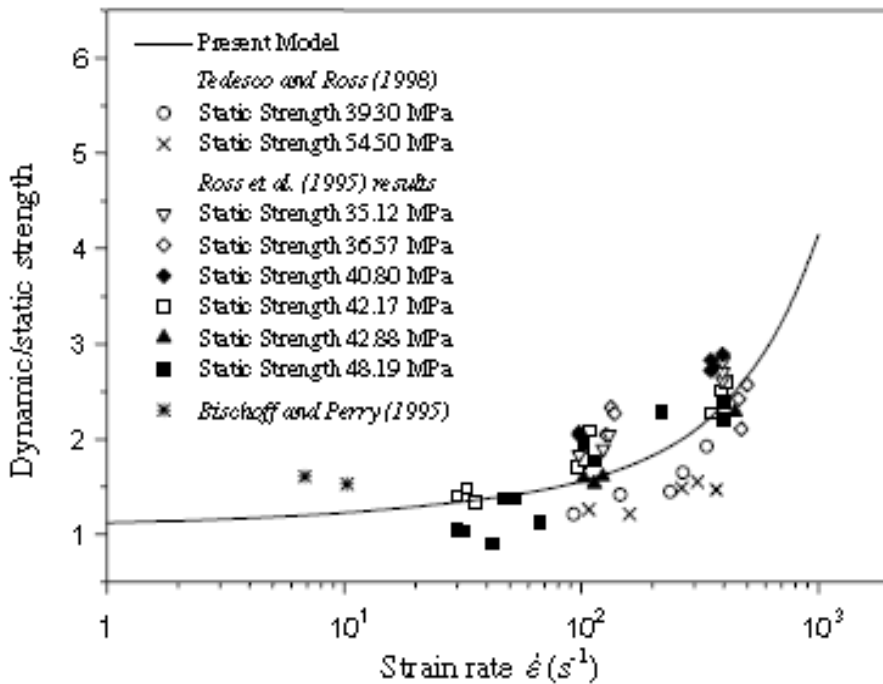


Figure 2-2: Normalized concrete compressive strength vs. strain rate. (Yong Lu, 2004).

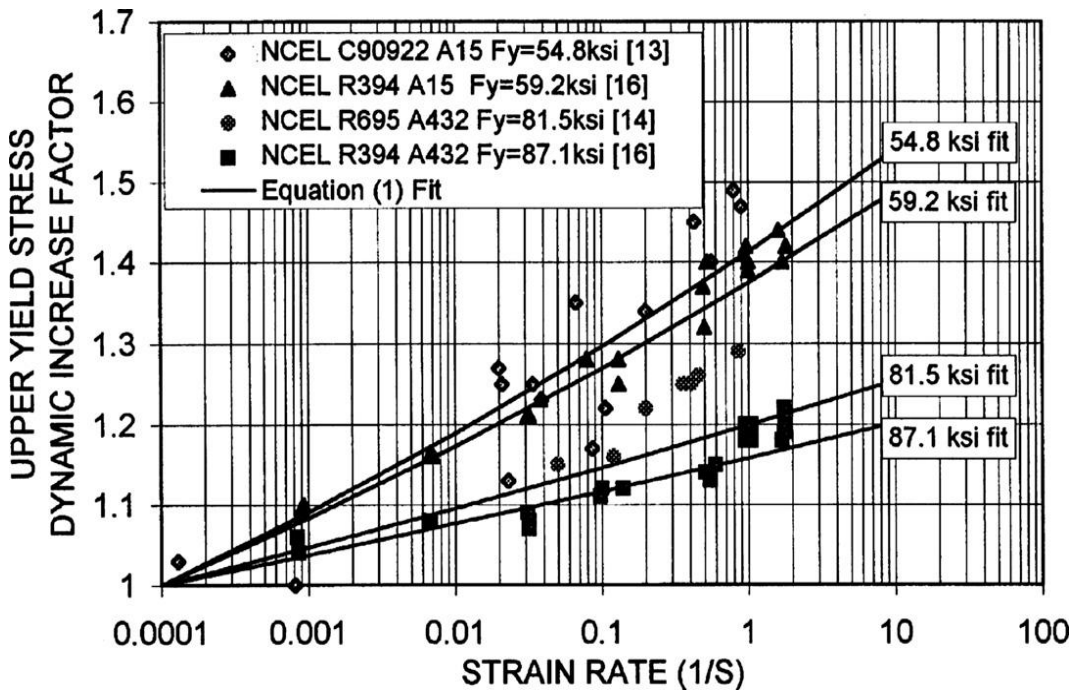


Figure 2-3: Effect of Strain Rate on Yield Stress of Steel Reinforcement (Malvar L. J., 1998)

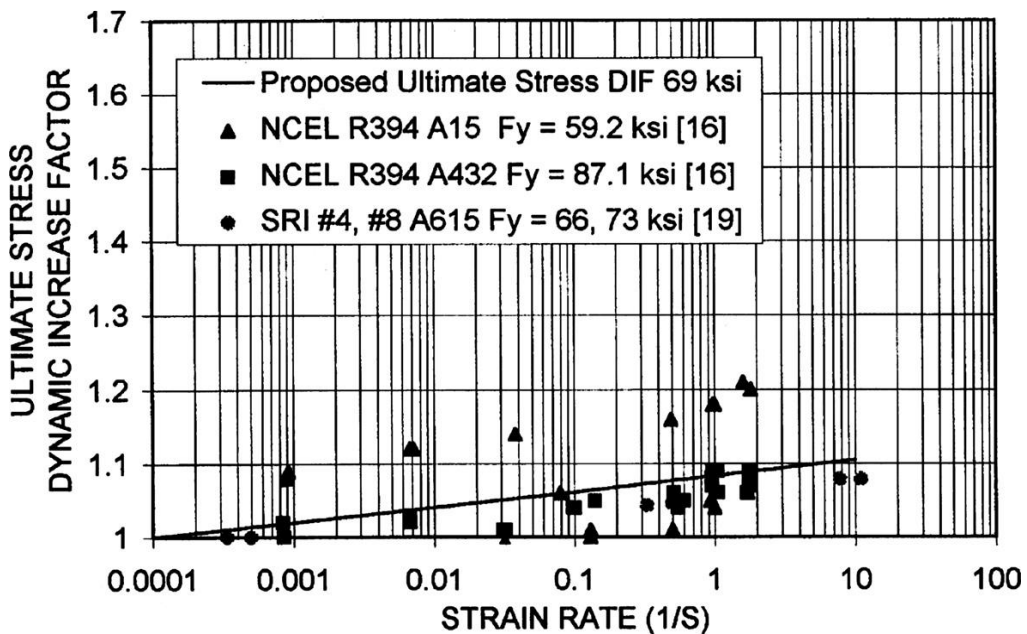


Figure 2-4: Effect of Strain Rate on Tensile (Ultimate) Strength of Steel Reinforcement (Malvar L. J., 1998)

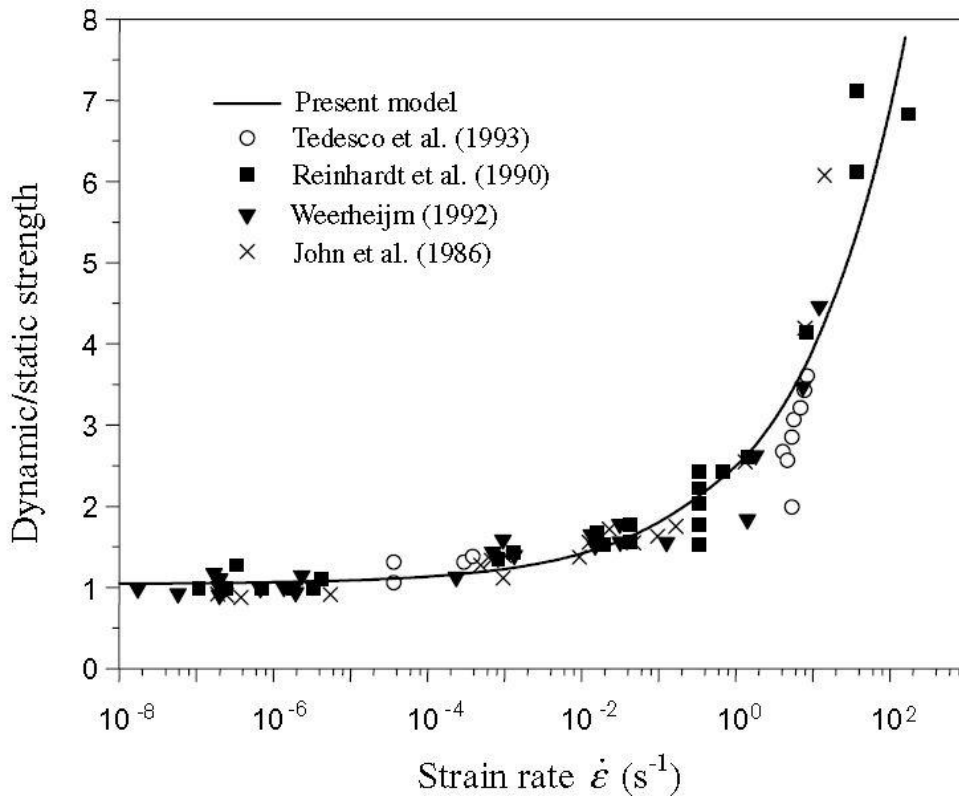


Figure 2-5: Normalized dynamic concrete tensile strength vs. strain rate. (Yong Lu, 2004)

UFC 3-340-02 (U.S. ARMY CORPS, December, 2008) provides guidance on the inclusion of strain-rate effects in the computation of component axial and flexural strength in the form of stress-increase factors. The UFC presents a simple equation (Equation 1) for strain rate, which is assumed to be constant from zero strain to the yield strain. The assumption of constant strain rate to yield is not unreasonable given the coarseness of the analysis that generally accompanies the use of the stress-increase factors.

$$\varepsilon^{\circ} = \frac{f_{ds}}{E \times t_e}$$

Where  $f_{ds}$  is the dynamic design stress which is function of minimum specified yield stress,  $E$  is the elastic modulus for steel and  $t_e$  is the time to yield the cross section.

Stress-increase factors, which are termed Dynamic Increase Factors (DIF) are used to designate the increase the yield stress and tensile strength of



structural steels. Complexity in analysing the dynamic response of blast-loaded structures involves the effect of high strain rates, the non-linear inelastic material behavior, the uncertainties of blast load calculations and the time-dependent deformations.

### 2.3 Rate of Damage

The rate of loading affects the response of concrete to dynamic loading. As concrete is a heterogeneous material with inherent microcracks, discontinuities and voids that are initially present in the material, its behavior during static uniaxial loading is affected by the propagation of internal microcracks, which are tensile in nature and primarily oriented in the axial direction. During rapid loading, the time available for microcrack development or propagation is reduced. Hence, the strain rate dependent behavior of microcracking can influence the response when concrete is subjected to the very high rates of loading that occur during impact (Bischoff and Perry 1991).

#### *The Stéfan Effect*

(Rossi, 1997) explains this effect as the physical mechanism involved in strain rate effects. It is explained as "When a thin film of viscous liquid is trapped in between two perfectly plane surfaces that are moved apart at a displacement rate  $\dot{h}$ , the film exerts a return force on the plates that is proportional to the velocity of separation". The mechanism is reflected by following equation:

$$F = \frac{3 \times \eta \times V^2}{2 \times \pi \times h^5} \times \dot{h}$$

Where, F is the return force,  $\eta$  is the viscosity of the liquid, h is the initial distance between two plates,  $\dot{h}$  is the velocity of separation of two plates ( $\dot{h} > 0$ ) and V is the volume of the liquid.

If we assume the presence of water in the concrete pores underlines a mechanism of this type when the solid matrix (here regarded as a network of plates) is subjected to tensile strains, it can be understood why loading rate effects are large in wet concretes and very small in dry concretes, Figure 2-5 (Li & Zheng, 2004). More ever, it has been shown that the absolute increase in tensile strength and in Young's modulus due to

rate effects is independent of the water cement ratio as in figure 5. Knowing that the diameter of the micropores of the hydrates is, unlike that of the capillaries, independent of the w/c ratio of the concrete, it is assumed that the micropores of the hydrates play a preponderant role in strain rate effects. The following figure illustrates the Stéfan Effect.

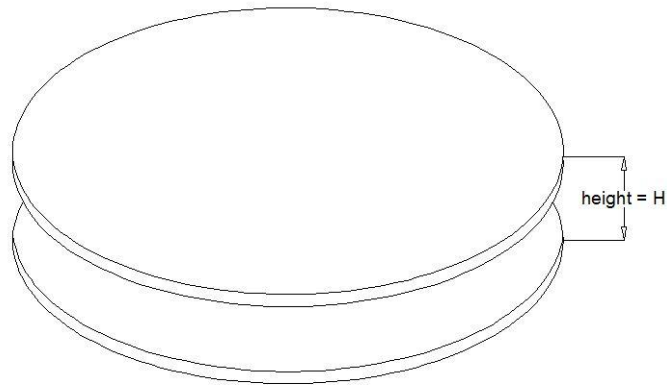


Figure 2-6: The Stefan Effect. (Li & Zheng, 2004)

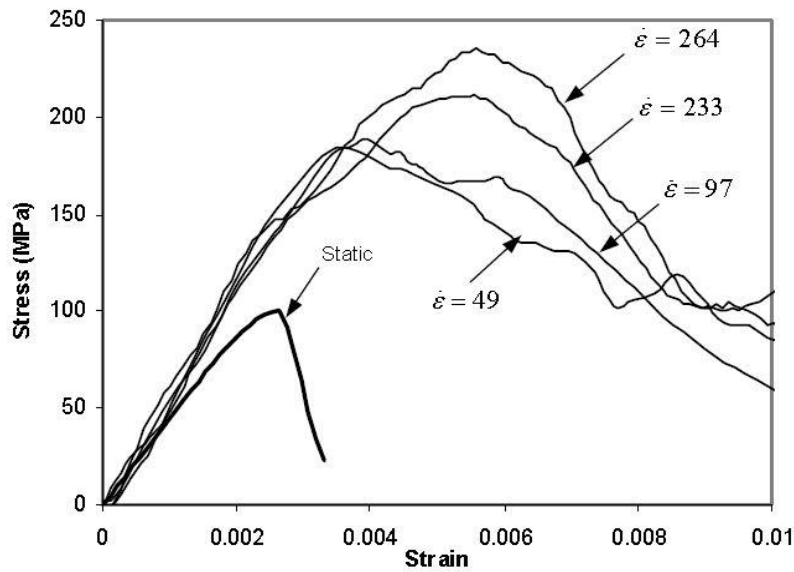


Figure 2-7: Stress-strain curves of concrete at different strain rates (Ngo, 2004)

## 2.4 Confinement Effect

Lateral inertia confinement also affects the strength enhancement of concrete at high rates of loading. According to Bischoff and Perry (Bischoff, 1991), an elastic material loaded in compression will expand in the transverse direction as a result of Poisson's ratio effect. However, a cylinder loaded rapidly in the axial direction will not

be able to expand instantaneously in the lateral direction because of inertial restraint, causing it to be initially in a state of uniaxial strain with corresponding lateral stresses that will act as a form of confinement (Bischoff, 1991). As concrete is sensitive to lateral confining pressure, even a small lateral confining pressure of 10 percent of the uniaxial compressive strength, can cause a 50 percent increase in the failure strength (Kotsovos, 1987). Since the lateral unloading velocity of brittle failure is considerably less than the axial elastic wave velocity, unloading could be sufficiently delayed for the increased compressive strength of the confined central core. Thus, due to insufficient unloading time, a cylindrical specimen will have a greater load-carrying capacity and thus an apparent strain-rate effect due to the inertia forces (Bischoff, 1991). The inertia forces have the consequence of opposing both the onset of microcracks and their propagation, thereby delaying micro-crack localization. Inertia also acts after the stage of crack localization, opposing the propagation of the macro-cracks. The rate of loading at which the lateral inertia confinement effect becomes significant is different from the rate of loading at which the strain rate effect causes strength enhancement. Even though the two effects act simultaneously, the Stefan effect and inertia forces are activated with different intensities according to the loading rate imposed on the specimen. For strain rates less than or equal  $1\text{s}^{-1}$ , an increase in material strength is related to viscous phenomena due to the presence of free water in the nanopores of concrete hydrates. For strain rates equal to or greater than  $10\text{ s}^{-1}$ , inertia forces are mainly responsible for increasing strength (Rossi 1997).

# CHAPTER 3: Evaluation of Dynamic Response in Concrete.

## 3.1 Introduction

The dynamic response of concrete is influenced by material strain rate effects which are attributed to limiting rate of damage propagation, visco-elastic response and Stefan effect. The combined influence of all these factors is to increase the modulus and strength obtained at higher strain rates. These effects are captured in the constitutive material models, which include several internal parameters to account for strain rate effects. The choice of the internal parameters often depends upon the basic formulation of the material constitutive model, which rely on plasticity, damage mechanics, viscoplasticity or a combination of these. These material models available in commercial finite element codes and are often calibrated using known data such that the user input is limited to providing known information about the material composition and quasi-static strength.

When concrete structural elements are subjected to transient compressive stress, the material response is also influenced by the level of confinement. Concrete is a pressure sensitive material and its material response is influenced by the level of confinement. While the material pressure sensitive material response is captured in the constitutive models, there is also dynamic confinement produced by inertial effects which is influenced by the geometry of the structure. The confinement of expansion of concrete under dynamic loading results in a differential level of confinement at different distances from the axis of compression. In predicting the response using dynamic finite element analysis, this geometric effect would be influenced by the element mesh size used in the analysis. The effect of mesh size and the confinement effects therefore need to be carefully evaluated.

In this chapter the influence of the following three factors (a) constitutive material model; (b) mesh size; and (c) confinement effect are investigated in a systematic way using a commercial dynamic finite element analysis software, LS-DYNA. LS-DYNA was chosen since it is currently used extensively for blast analysis of structures. In this study, three constitutive material models available within LS-DYNA were chosen for evaluation. Concrete cylinder specimens with three different sizes were used in

evaluating the dynamic response when subjected to a prescribed velocity or strain rate. Evaluation of the global response parameters and the local material level response were performed using different mesh sizes and four different prescribed strain rates.

## **3.2 Background**

In this study, simulations were performed for three material models for three different sizes of cylindrical specimens considering two different mesh sizes. The three material models available in LS-DYNA used in the analysis were: a) Mat\_72R3 (Karagozian and Case) model, b) Mat\_84 (Winfrith concrete) and c) Mat\_159 (CSCM model). A brief description of the three material models and the internal material parameters of each is provided in the following.

### ***3.2.1 Mat\_72R3 (Karagozian and Case model)***

The Karagozian and Case (K&C) model was developed by Geotechnical and Structures Laboratory of US Army Engineering Research and Development Center (ERDC). The model was calibrated for concrete with unconfined compressive strength obtained by testing cylindrical specimens equal to 45.6 MPa, which is commonly used by many numerical simulations as standard concrete. The default parameters for K&C model have been calibrated using well characterized concrete for which all the necessary data was available. The uniqueness of this model is that, it requires input value for just the unconfined uniaxial compressive strength ( $f_c'$ ). The other parameters are taken as for the default value (which can be changed if the data is available). More information about this model can be found in LS Dyna Theory manual (Dyna, LS-DYNA Theory Manual, March 2006).

In this study, the mass density of concrete was set equal to  $2.32 \times 10^{-9}$  Mg/mm<sup>3</sup>, the Poisson's ratio was set to 0.2, the uniaxial compressive strength was 45.4 MPa and the uniaxial tensile strength was set to 4.75 MPa and maximum aggregate size was set to 19 mm. Simulations were run with both rate effects on and off, hence the value of compressive strength for this material was selected as 45.4 MPa, in order to allow the usage of the effective strain rates published in LS Dyna Keyword manual (Dyna, LS Dyna Keyword manual). The

72R3 concrete model does not provide direct way to turn strain rate on or off. Instead, user is required to define and include the strength enhancement versus strain rate curve in the program. LS Dyna has a predefined strength enhancement curve for concrete provided in (Dyna, LS-DYNA Theory Manual). The values used are as shown below:

Strain rate (1/s)	-3E+04	-3E+02	-1E+02	-3E+01	-1E+01	-3E+00	-1E+00	-1E-01	-1E-02	-1E-03	-1E-04	-1E-05	0E+00
Strength Enhancement	9.7	9.7	6.72	4.5	3.12	2.09	1.45	1.36	1.28	1.2	1.13	1.06	1

Table 3-1: Tensile strength enhancement versus strain rate for Mat\_72R3 (Dyna, LS-DYNA Theory Manual)

Strain rate (1/s)	0E+00	3E-05	1E-04	1E-03	1E-02	1E-01	1E+00	3E+00	1E+01	3E+01	1E+02	3E+02	3E+04
Strength Enhancement	1	1	1.03	1.06	1.14	1.2	1.26	1.29	1.33	1.36	2.04	2.94	2.94

Table 3-2: Compressive strength enhancement versus strain rate for Mat\_72R3 (Dyna, LS-DYNA Theory Manual)

### 3.2.2 Mat\_84 (Winfrith Model)

Winfrith Concrete model is a plasticity-based model which considers the shear failure surface proposed by Ottosen in 1977. This model was developed by Broadhouse and Neilson (Broadhouse, October, 1987). Winfrith concrete model offers an option to include or exclude the strain rate effects, and to include smeared reinforcement. It is a basic plasticity model that includes the third stress invariant for consistently treating both triaxial compression and triaxial extension, like Mohr-Coulomb behavior. More information about this model can be found In LS Dyna theory manual (Dyna, LS-DYNA Theory Manual, March 2006).

In this study, the mass density was set to  $2.32 \times 10^{-9}$  Mg/mm<sup>3</sup>, the initial tangent modulus of concrete was set to 31,877 MPa and the Poisson's ratio 0.2. The uniaxial compressive strength was 46 MPa and uniaxial tensile strength was 4.75 MPa. Also, maximum radius of the aggregate was set to 9.5 mm and the fracture energy (energy dissipated in opening a crack) as read from CSCM concrete output is 0.0922 N.mm/mm<sup>2</sup>. The strain rate is incorporated in the Winfrith concrete model through parameter 'RATE'. The simulations are run with both, strain rate on and off.

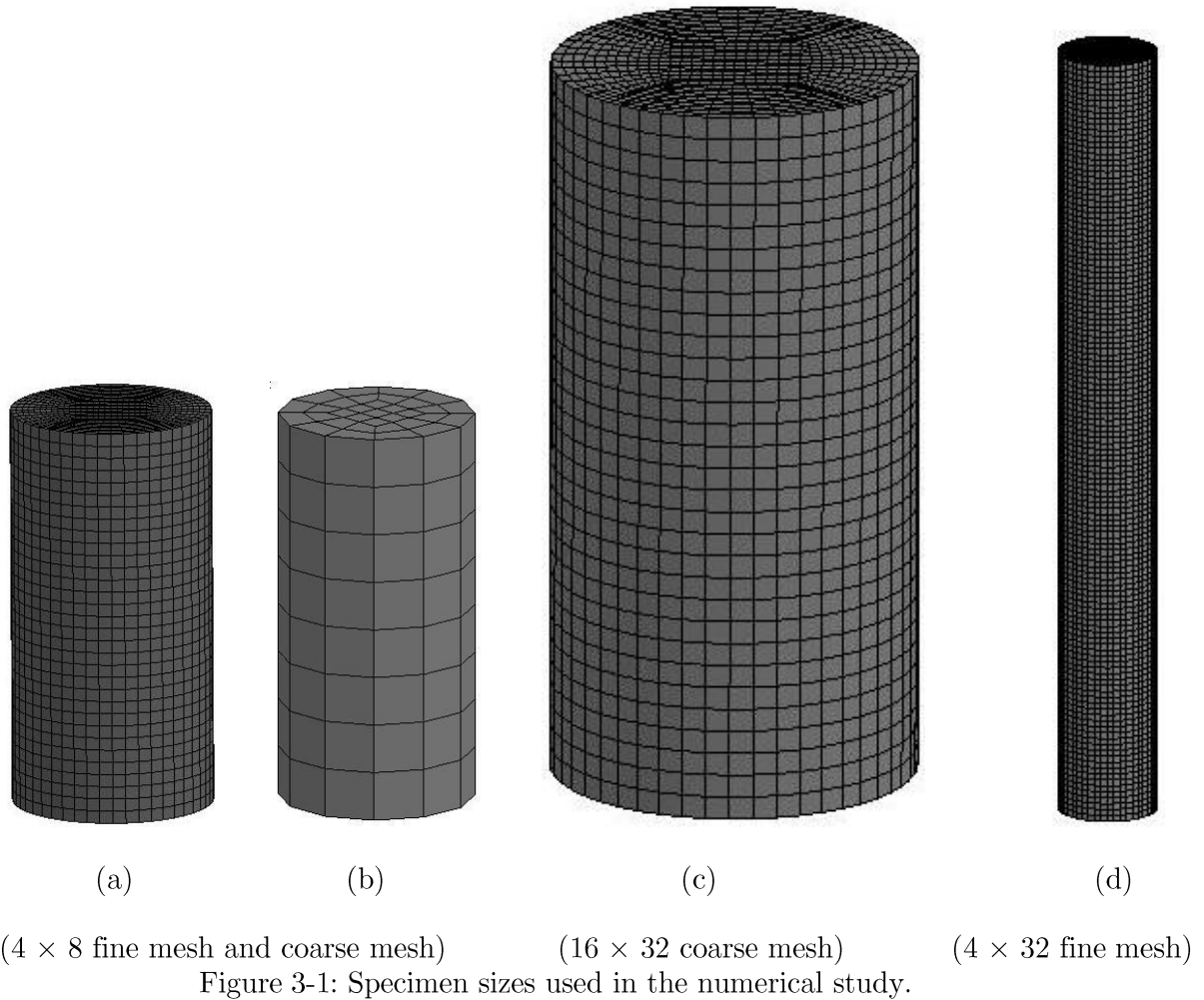
### 3.2.3 Mat\_159 (CSCM Concrete model)

CSCM concrete (or continuous surface cap model) was developed by Roadside safety applications to develop concrete material model for use in roadside safety simulations, implement model in LS Dyna finite element code and evaluate the model against available test data. It was developed to predict the dynamic performance, both elastic deformation and failure of concrete used in safety structures when involved in collision with a motor vehicle (Murray, May 2007). This model is a cap model with a smooth or continuous intersection between the failure surface and the hardening cap. This surface uses a multiplicative formulation to combine the shear surface with the hardening compaction surface smoothly and continuously. The continuous surface cap model is available for solid elements in LS-DYNA. The user has the option of inputting the user-defined material properties, or requesting default material properties for normal strength concrete.

In this study, following parameters were input to generate default material properties from normal concrete. The unconfined compressive strength was set to 46 MPa, maximum aggregate size was set to 19 mm and mass density was set to  $2.21 \times 10^{-09}$  Mg/mm<sup>3</sup>. The erosion parameter was set to 1.1 so that material erodes when the value of principal stress surpasses value of 0.1. For CSCM model, LS Dyna has parameter IRATE to include or exclude the strain rate effects.

### **3.3 Numerical Simulation**

Dynamic simulations were performed for concrete cylinders with prescribed velocity at one end while the other end was kept fixed against all displacement. Three specimen sizes were chosen for evaluating the geometric confinement effect and the influence of mesh size. The following specimens were used: 4 in  $\times$  8 in (101.6 mm  $\times$  203.2 mm) b) 4 in  $\times$  32 in (203.2 mm  $\times$  203.2 mm) and c) 16 in  $\times$  32 in (406.4 mm  $\times$  812.8 mm). The cylinder sizes were based on the standard cylinders used for obtaining compression strength results. Evaluations of the three material models and the influence of mesh size on the predicted response were conducted using the 4in x 8in cylinders. The inertial confinement effect which is one of the causes of strength enhancement at high loading rates is studied using the 16in x 32in and 4in x 32in cylinders. The cylinder specimens were meshed using the 8-noded solid elements and simulations were run with two mesh sizes: a) coarse mesh (seed dimension = 1 in.) and b) fine mesh (seed dimension =  $\frac{1}{4}$  in.) as shown in the figure below.



### 3.3.1 Boundary and Loading conditions

The top nodes were restrained against in-plane translation in the X and Y directions, so as to allow translation in the axial direction (Z direction). The bottom nodes were restrained against all translation. Although the solid elements do not have rotational degree of freedom, restraining the translation of nodes imitates a fixed support condition. The boundary condition is provided using the SPC (Space point constraint) command in LS Prepost.

The concrete cylinders are subjected to dynamic compressive velocity loads to produce prescribed strain rates equal to 0.0125/s, 1/s, 10/s, and 100/s. The range selected covers the rates of loading occurring during structural vibration, earthquake, impact and blast. The loading was defined using the ‘prescribed motion set’ under \*boundary in LS Prepost. The finite element model showing the prescribed boundary



and velocity boundary conditions is shown in Figure 3.2. The velocity prescribed at the loaded end was calculated to obtain the prescribed strain as

$$\text{Strain rate} = \frac{\text{Prescribed velocity}}{\text{Depth of cylinder}}$$

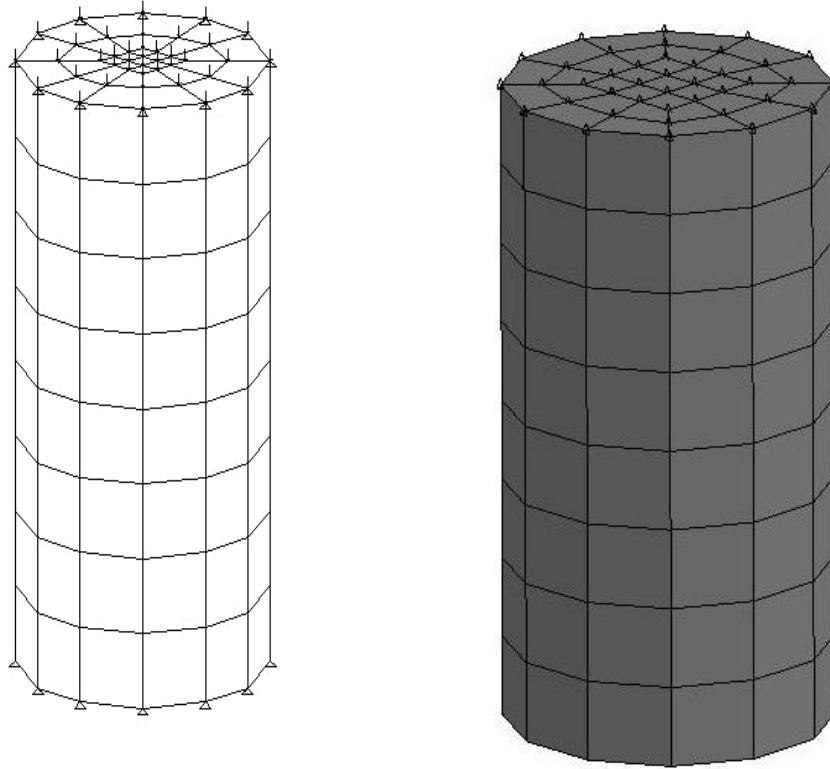


Figure 3-2: Boundary and loading conditions

The various elements within model respond differently and at different time for the applied dynamic load. To have a stress-strain curve that represents response of the whole model, the response of the elements at mid-height plane of cylinder is considered for reporting the stress and strain values. The average force on a cross section was obtained using the ‘*secforc*’ function in LS Prepost. The average stress was then calculated by dividing the force by initial cross sectional area. The displacement was obtained from the history plot in LS Prepost. The history of nodes provides the total displacement of the nodes. To find the displacement of mid height section, the average vertical displacement was calculated for nodes located at the mid-section. The average strain was then determined by dividing the average mid-height displacement by half height of cylinder. During the dynamic analysis both the stress and strain were calculated at same time step to obtain the continuous evolution of stress-strain response.

### **3.4 Results of Numerical Analysis**

In the first part of analysis the effect of mesh size is evaluated using the 4in x 8in cylinder specimen. These results were used to determine the mesh size used in evaluating the material models and confinement effect.

#### ***3.4.1 The effect of mesh size on concrete models***

The following are the results that have been drawn from various simulations considering a coarse mesh and a fine mesh. The seed dimension of coarse mesh = 1 inch (25.4 mm) and seed dimension of fine mesh = 1/4th of inch (6.35 mm). The results of the analysis for 0.0125/s, 1/s, 10/s and 100/s are shown in Figures 3-3, 3-4, 3-5 and 3-6, respectively. As a general observation there was a significant increase in the computational time using the fine mesh when compared to the fine mesh. The findings pertaining to the influence of mesh size can be summarized as below.

1. For rates of loading up to 10/s, the linear response predicted using both the fine and the coarse meshes are identical for both CSCM and 72R3 models. There is a divergence in the predicted responses with the onset of nonlinearity. At 100/s both models predict different stiffness in the initial linear response.
2. For the CSCM model the response obtained from a fine mesh predicts a higher strength and a less brittle response at all rates of loading. The predicted response exhibits a strain softening response at all rates of loading, except at 0.0125/s the

finer mesh predicts no strength degradation with continued straining. The strain corresponding to peak stress is lower for the coarser mesh.

3. Both CSCM and 72R3 material models predict a higher strength and slower rate of strength decrease in the post-peak for the finer mesh. The finer mesh predicts a higher stress and a larger strain at peak stress. The peak stress for both meshes do not differ more than  $\pm 8\%$ .
4. There is a good correspondence between the predicted responses for both mesh sizes at 1/s and 100/s for the CSCM and 72R3 models, respectively. This suggests that the models provide mesh independent behavior at these two different rates of loading; at these rates of loading the average stress predicted by the material model is equal to average strain predicted by the mid-height deformation for both mesh sizes.
5. At 100/s both CSCM and 72R3 predict strains at peak stress in the range of 0.01, which are an order of magnitude higher than the quasi-static strain at peak stress. This indicates that the total deformation in the cylinder is significantly higher than the quasi-static response.
6. For both low and high strain rates, a considerably higher strength and a load response which is not consistent with experimental observations is obtained for the Winfrith concrete model. There is also a large divergence between the predicted response for the coarse and fine meshes for this material model.

The observed difference in the peak stress and the corresponding strain obtained from a finer mesh for the CSCM and 72R3 models can be explained considering localization of damage. In smaller mesh the influence of localized damage would be confined to a smaller volume restricted to fewer elements. The average strain in this case would be higher than the average strain where a larger volume of the material experiences damage due to larger elements.

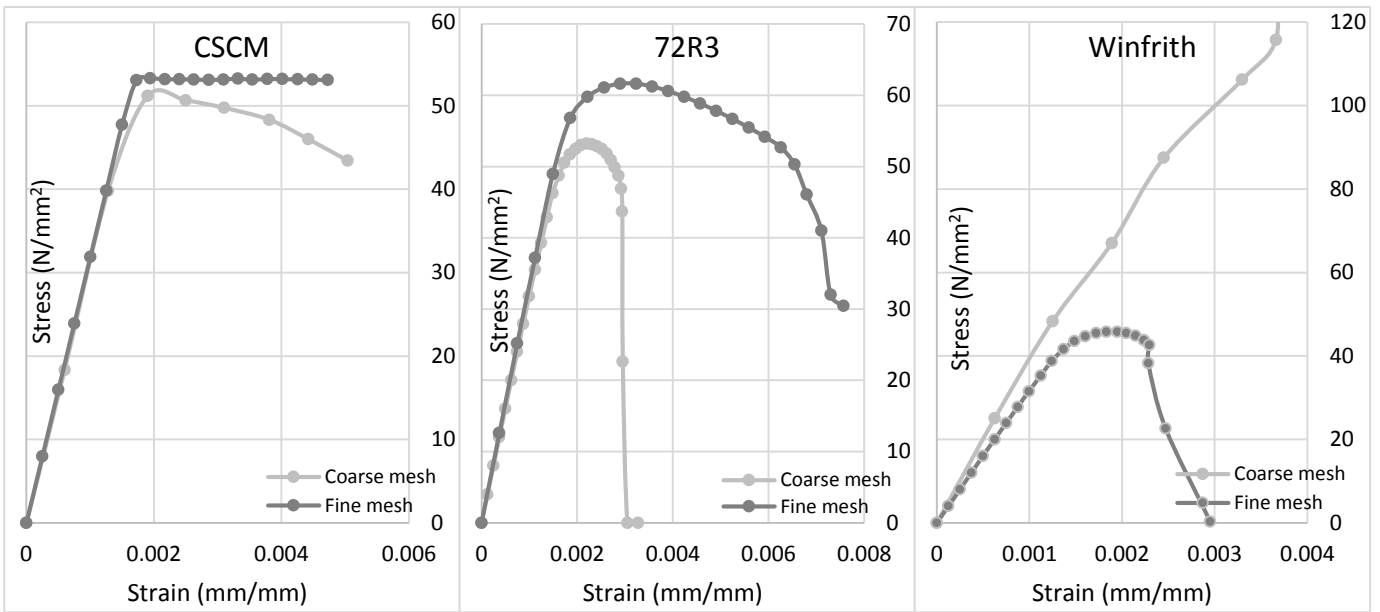


Figure 3-3: Influence of Mesh size on the predicted response at 0.0125/s

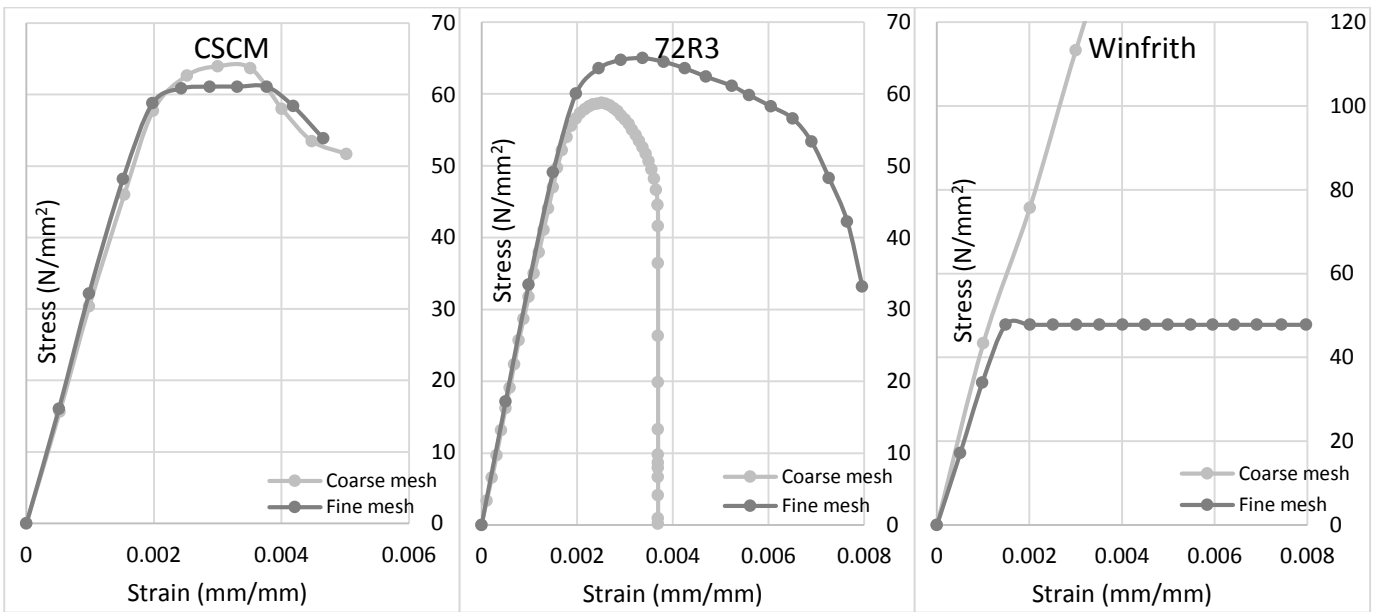


Figure 3-4: Influence of Mesh size on the predicted response at 1/s

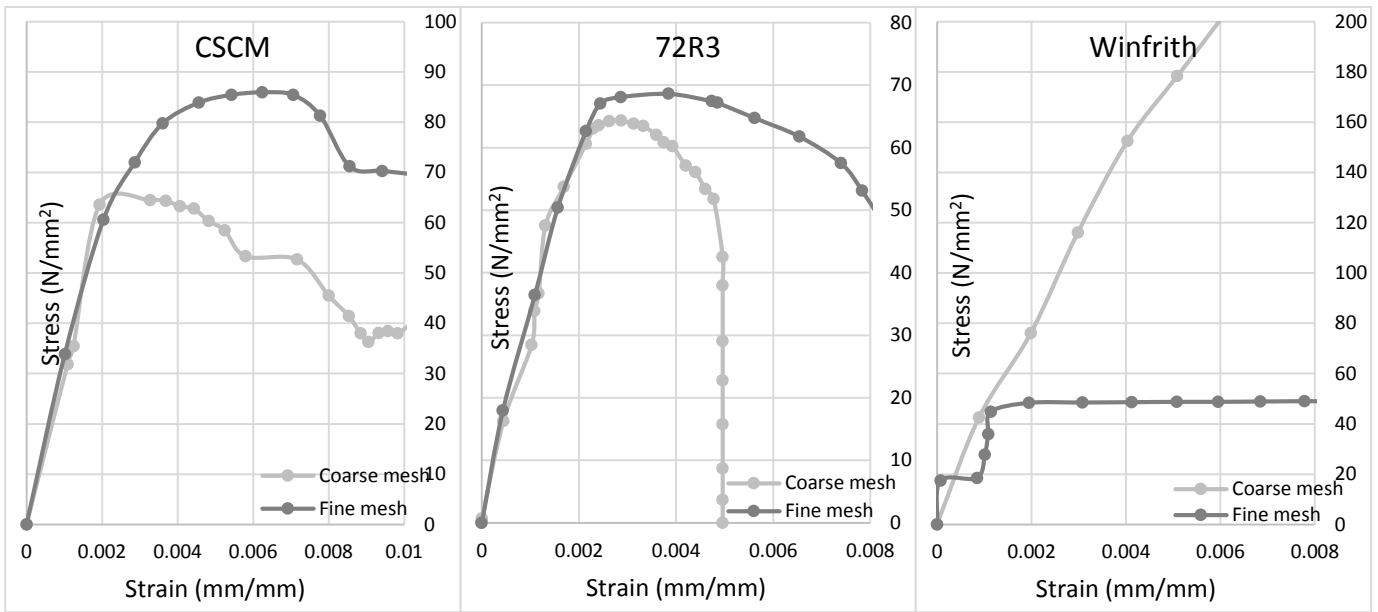


Figure 3-5: Influence of Mesh size on the predicted response at 10/s

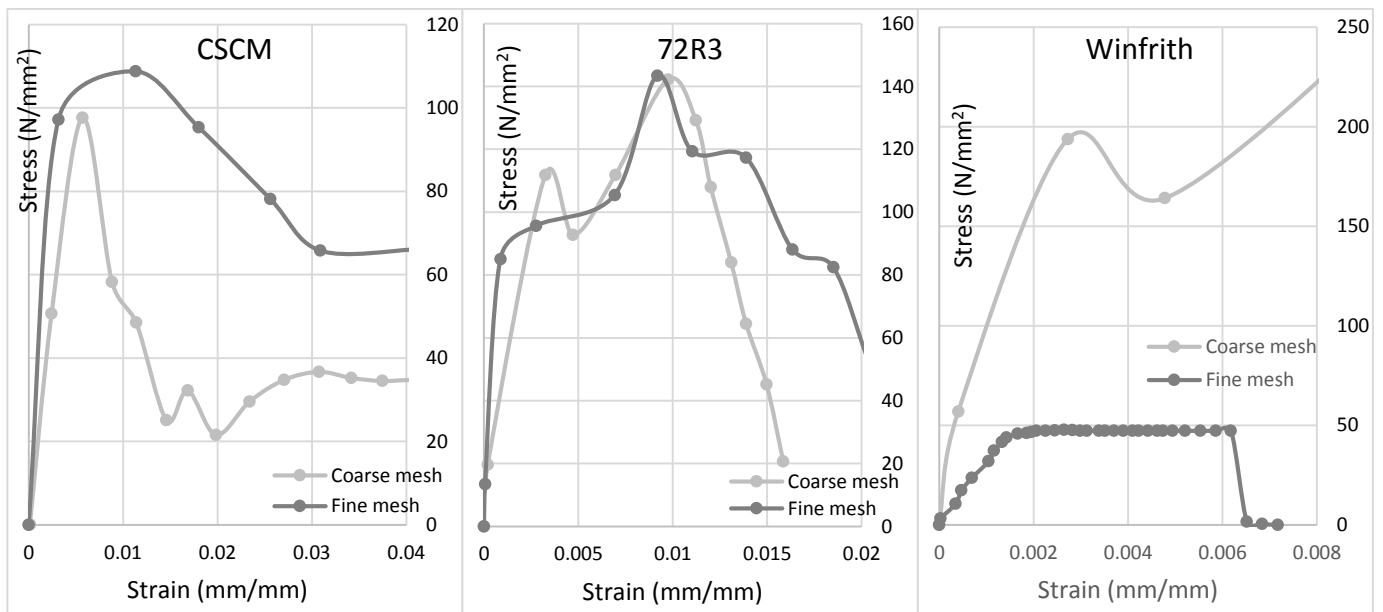


Figure 3-6: Influence of Mesh size on the predicted response at 100/s

### 3.4.2 Comparison of material models

Comparison of the predictions of the three material models were performed for the 4in × 8in cylinder using the coarse mesh and are shown in Figure 3-7. The findings pertaining to predictions of the different material models are summarized below.

1. For lower strain rates, the material models predict similar behavior. The initial linear response predicted by all three models is identical. The average stress strain response deviates with the onset of non-linearity.

2. The CSCM model predicts a residual strength even for all strain rates, which is consistent with the formulation of the model.
3. The Winfrith concrete model predicts an almost perfectly plastic response at 1/s and 10/s. At 100/s the model predicts inconsistently high stress, which are not in consistent with established experimental observations.
4. The CSCM and 72R3 models predict comparable response at all strain rates. A rise in the stress level at higher strain rates, which is consistent with the experimental observations.

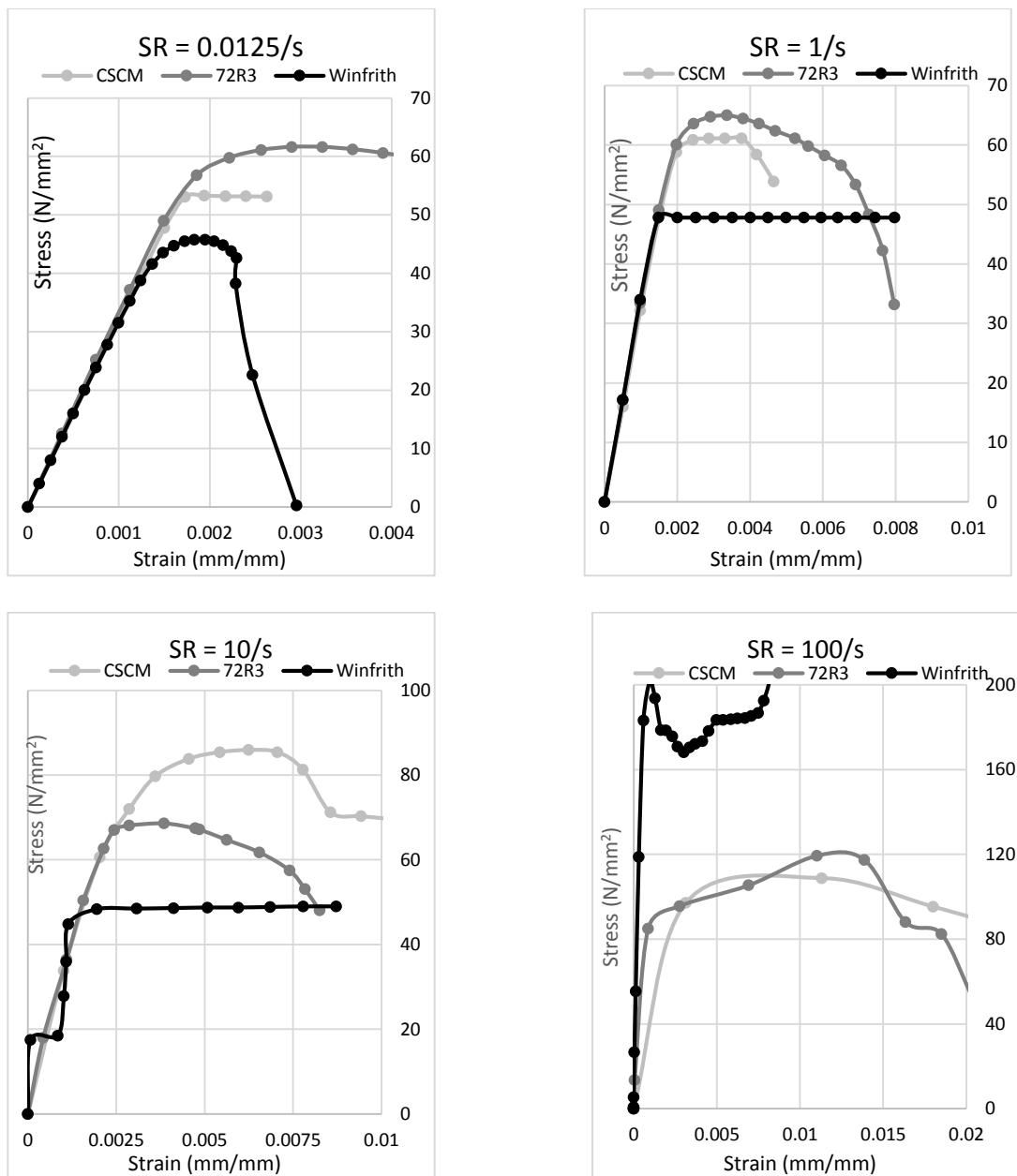


Figure 3-7: Comparison of material models for various strain rates

### 3.4.3 Material Strain rate effect (load response)

The in-built strain rate effect available in the material models are evaluated by comparing the predictions with and without the option. A comparison between the predicted average stress-average strain response at 0.0125/s and 100/s for CSCM and 72R3 models is shown in Figure 3-8 and Figure 3-9. The findings on the strain rate effects are as below.

1. The general shape of the average stress response is similar with and without the strain rate effects. However, as the strain rate increases, there is a significant increase in the peak value of the stress. Also, we see a change in the model behavior at high strain rates.
2. There is an increase in the peak stress even without the strain effect option turned on. This corresponds to an increase in the resistance from inertial effects. Further increase in the peak stress with the strain rate option corresponds to the increase in material resistance, which contributes to an increase in the dynamic strength as captured in the constitutive material model. The results further indicate that even at 0.0125/s there is an increase in the material strain rate effect.

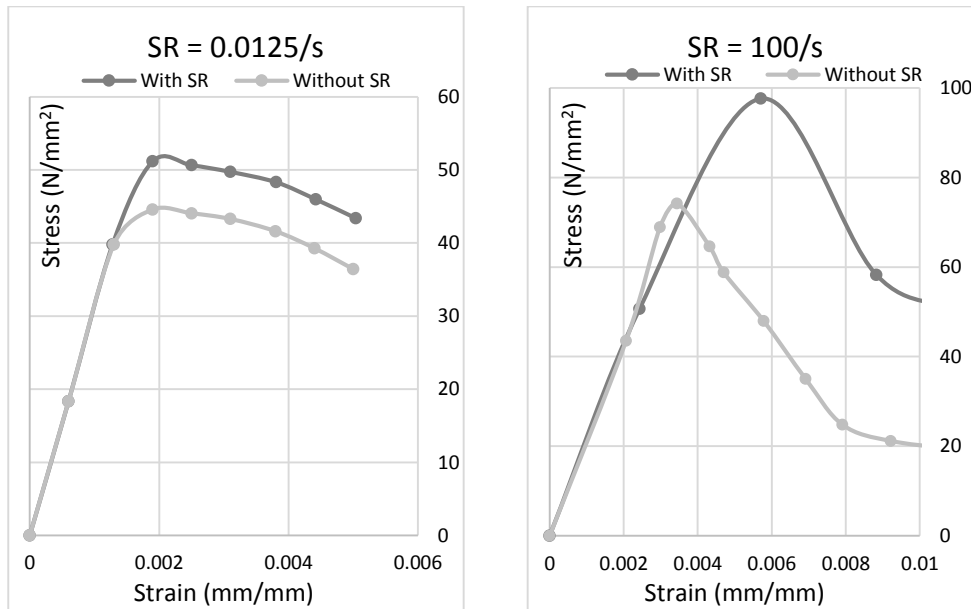


Figure 3-8: Comparison of inclusion and exclusion of rate effects for various strain rates in CSCM model.

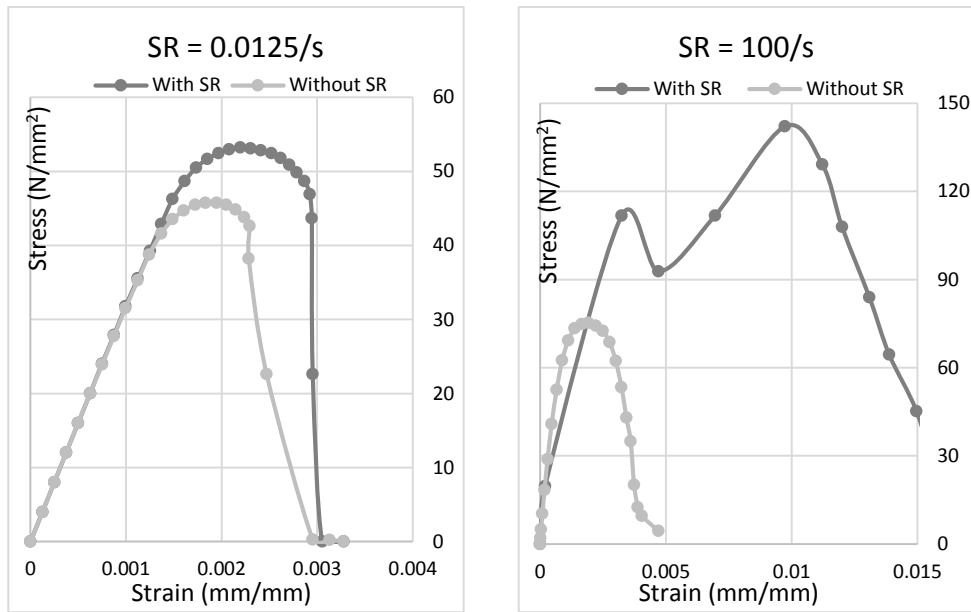


Figure 3-9: Comparison of inclusion and exclusion of rate effects for various strain rates in 72R3 model.

The results of the numerical analyses are now used to arrive at a choice of mesh size and material model.

1. The 25mm mesh size provides an ideal compromise between accuracy and computational speed.
2. CSCM and 72R3 material models provide reasonable predictions of the average stress response for prescribed velocity loading conditions, which are in agreement with each other.

In the subsequent evaluation, 1 in mesh size and CSCM and 72R3 models are used.

### 3.5 Material strain rate effect (Material response)

Stress histories at three different locations along the axis of the cylinder corresponding to  $Z = 5$  in, 16 in, and 27in for different applied strain rates were obtained. The locations along the length are shown marked in Figure 3-10. A comparison of stress histories predicted by 72R3 and CSCM models for 1/s are as shown in figures Figure 3-11, (a), (b) and (c) respectively. There is a gradual built up of stress at different locations upto a critical threshold value corresponding to 60MPa for 72R3 following which the material fails completely. Material failiure is indicated by decrease of stress to zero value. A close-up of stress build up is shown in Figure 3-13. Distinctive steps can be seen in stress build-up, which correspond to multiple reflections of the



stress wave in the cylinder superimposed over increasing stress produced by applied velocity at one end. The time period of steps in the response is approximately equal to  $4 \times 10^{-4}$  seconds. Similar response is produced by CSCM upto a maximum stress of 60 MPa. However, CSCM model produces a residual stress after attaining peak stress, which is inherent in the constitutive relations of material model. The close-up of stress build up also indicates a stepwise increase with step spacing equal to  $4 \times 10^{-4}$  seconds.

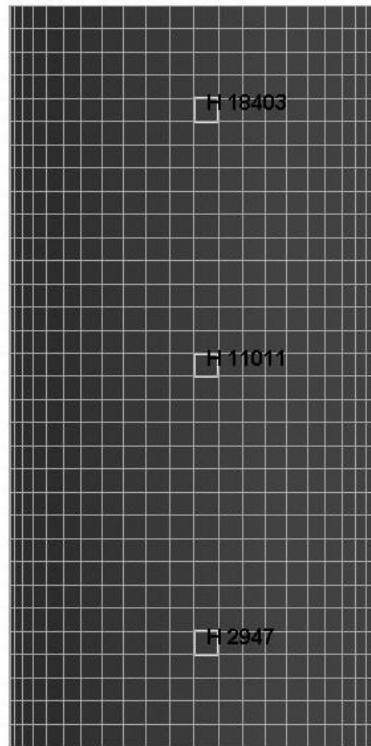


Figure 3-10: The position of load histories plot on the columns

A comparison of stress histories predicted by 72R3 and CSCM models for 10/s are as shown in figures Figure 3-11 (a),(b) and (c) respectively. The stress history indicates a rapid build up of stress upto 70MPa, within the first passage of compression wave. The passage of compression wave can be identified from the first peaks in stress history at the three locations. There is a decrease in amplitude of the peak stress as the compression wave propagates through the material. Following the passage of first compression wave there is unloading. This indicates that the initial stress built up compresses material into post peak. Subsequent changes in the stress are produced by reflected pressure from fixed end and continued loading from the prescribed velocity at the loaded end. As strain from prescribed boundary conditions continues to increase, the material resistance decreases with increase in strain. This is evident in the softening behaviour after the first peak. The reflected stress wave from the bottom causes a

further stress increase which eventually leads to failure. Similar response is also obtained from CSCM except that the material model predicts residual stress.

A comparison of stress histories predicted for 72R3 and CSCM models for 100/s are as shown in figures Figure 3-11(c) and Figure 3-12 (c), respectively. The stress history at the three locations indicates a very rapid built up to 242 MPa within a time of  $6.7 \times 10^{-5}$  seconds. The passage of first compression wave produces total failure in the material. The stress transmitted to the subsequent material points is lower. The material at  $y = 203.2$  mm fails before the stress pulse reaches mid height at time =  $19.93 \times 10^{-5}$  seconds. The results indicate total crushing of the material produced by the first stress wave. Similar response is predicted by CSCM model, except the stress amplitude produced by the first compression wave is 120 MPa, which is significantly smaller than the stress amplitude produced by 72R3 model.

First passage of compression wave produces a stress rise of 60 MPa for 1/s, 65 MPa for 10/s and 120 MPa for 100/s. It appears that the stress response produced by 72R3 and CSCM are nominally similar. There are however, differences in the rate of stress built up, maximum stress attained and post peak behavior. The stress waves in the 72R3 propagates a little early than that in CSCM model.

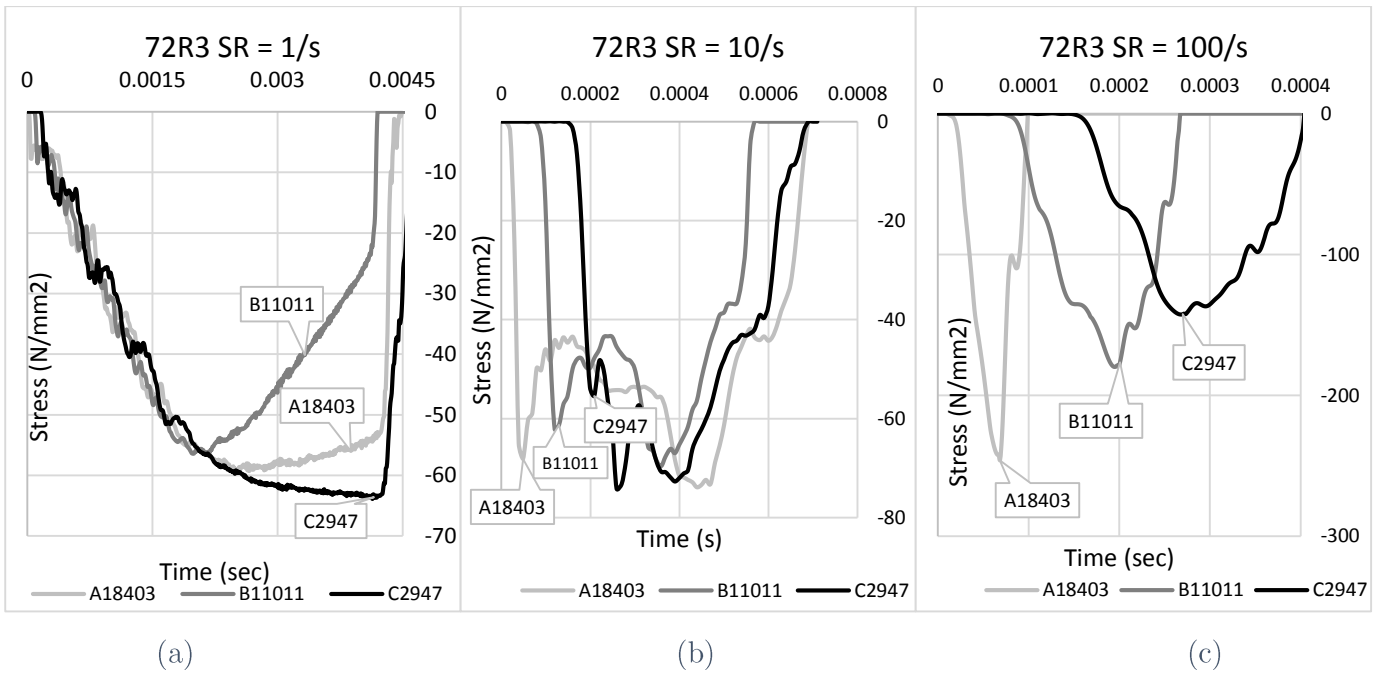


Figure 3-11: Comparison of stress histories predicted by 72R3 model for various strain rates.

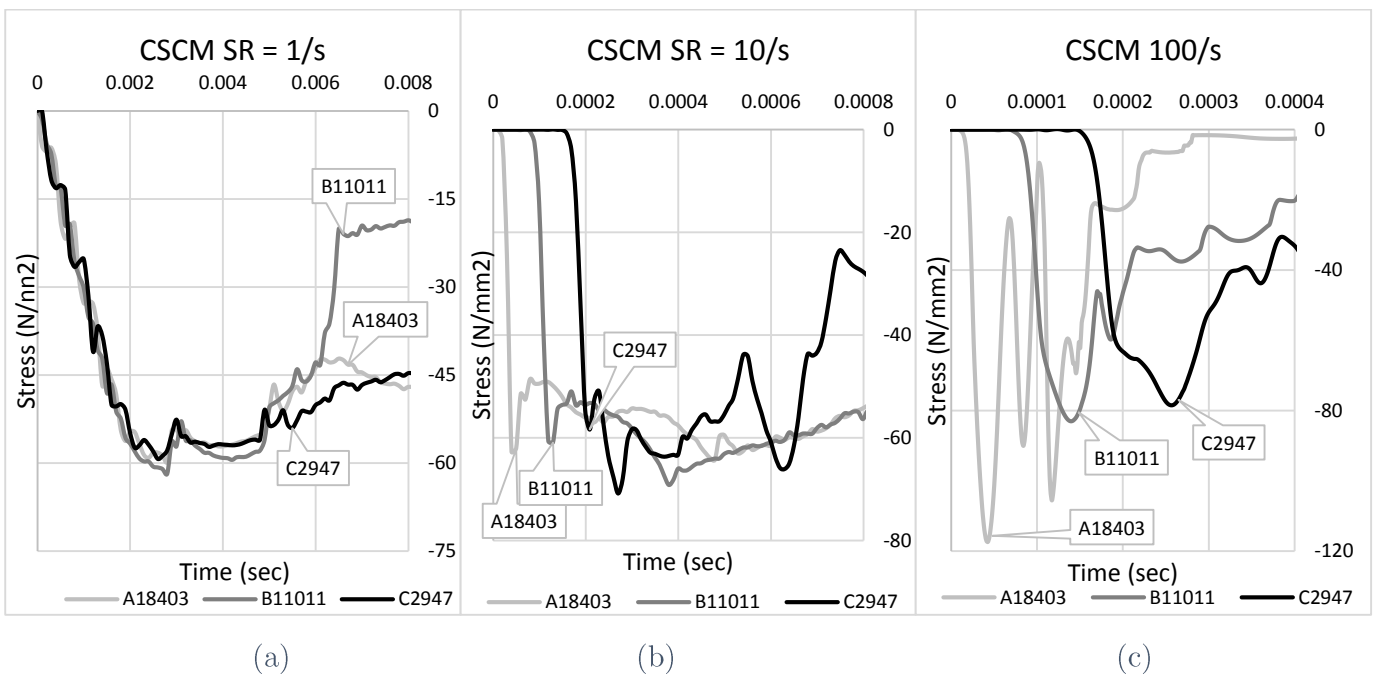


Figure 3-12: Comparison of stress histories predicted by CSCM model for various strain rates.

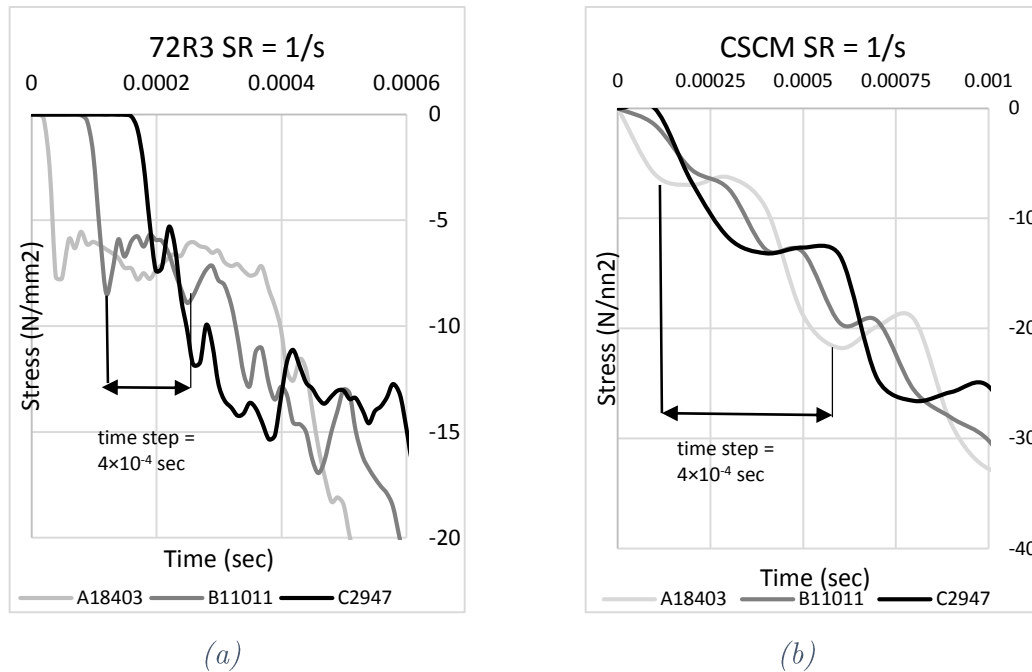


Figure 3-13: A close up graph of the stress built up in both the material model at strain rate of 1/s. Note the time step of the peaks

### 3.6 Evaluation of Confinement Effect

To study confinement effect a comparative evaluation of stress histories obtained from cylinders with two different diameters was performed. The strain rates considered are 1/s, 10/s and 100/s. Stress histories along a diameter at a cross section located at half height i.e. 406.4 mm from top, for the 4in x 32 in cylinder and the 16in x 32 in cylinder are shown as in *Figure 3-14*. In the 4in (100mm) cylinder the effect of inertial confinement is clearly evident in both the linear wave propagation and the non-linear material response found respectively at 1/s and 10/s rates of loading. Comparing the response from the 4in and the 16 cylinders it is clear that significantly higher stresses are produced in the cylinder with a larger diameter. The larger stresses could be attributed to higher level of confinement due to larger inertia in the radial direction. Further, the effect of confinement from the in-plane constrained motion at the boundary is more significant in the 16in cylinder than in the 4in cylinder at the same distance from the end.

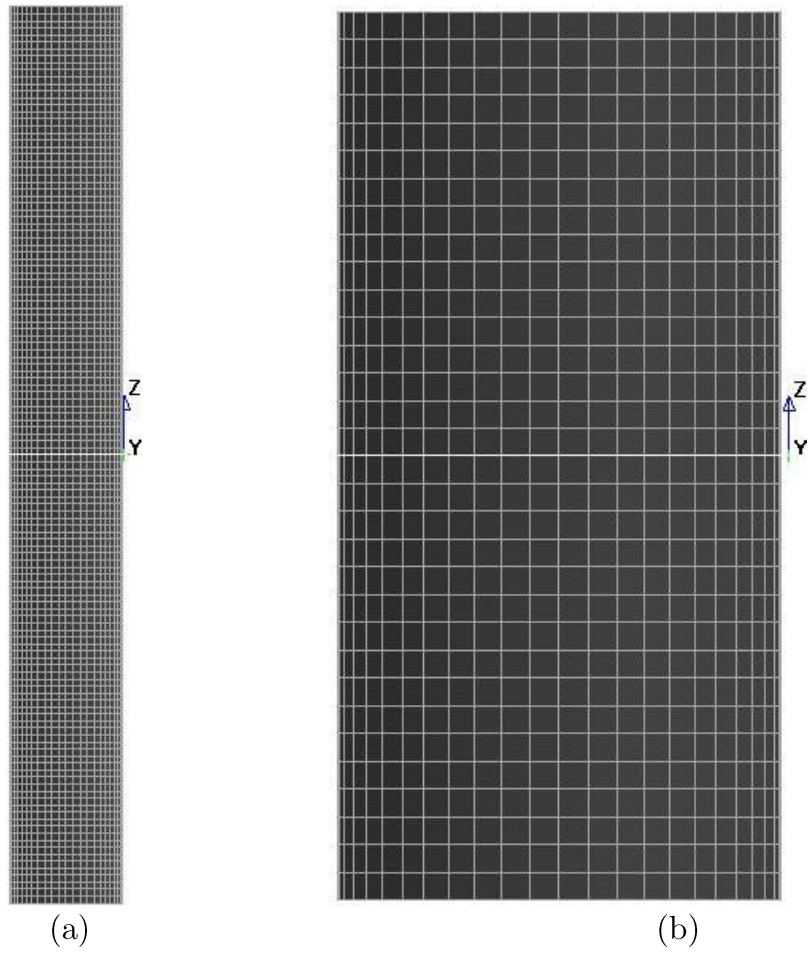


Figure 3-14: The section at which stress histories along the diameter are plotted in the 4in  $\times$  32in and 16in  $\times$  32in columns.

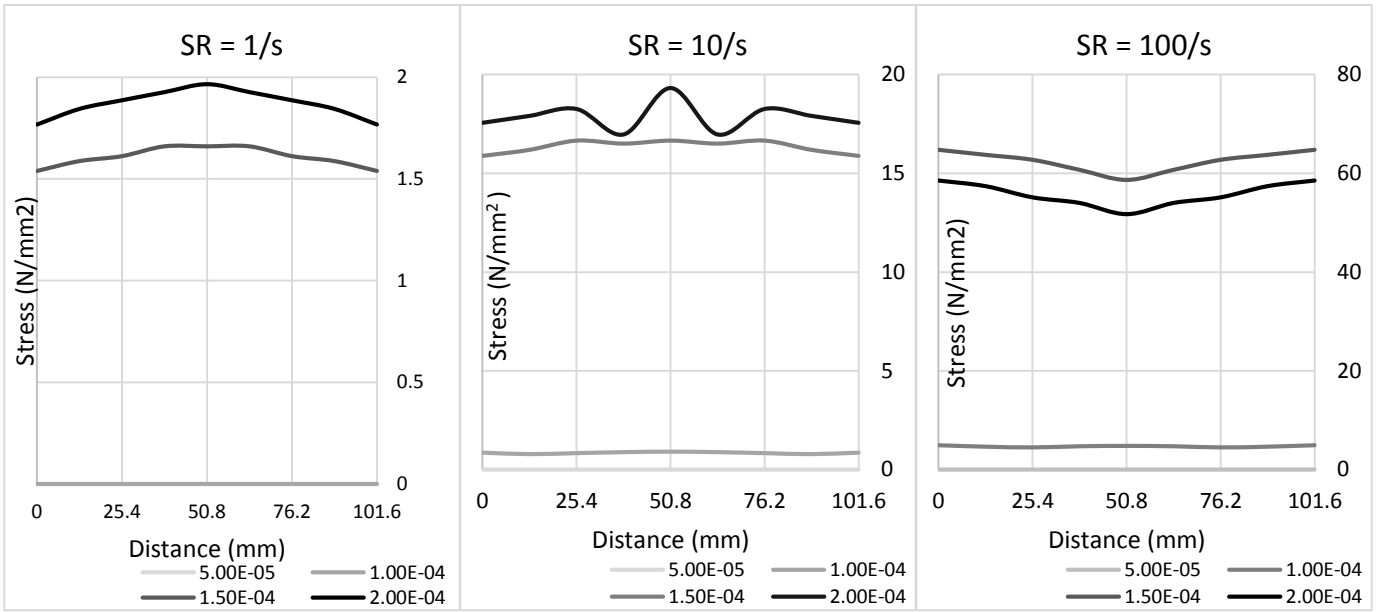


Figure 3-15: Stress history along diameter for 4 × 32 inches 72R3 column at half height for various strain rates at various times.

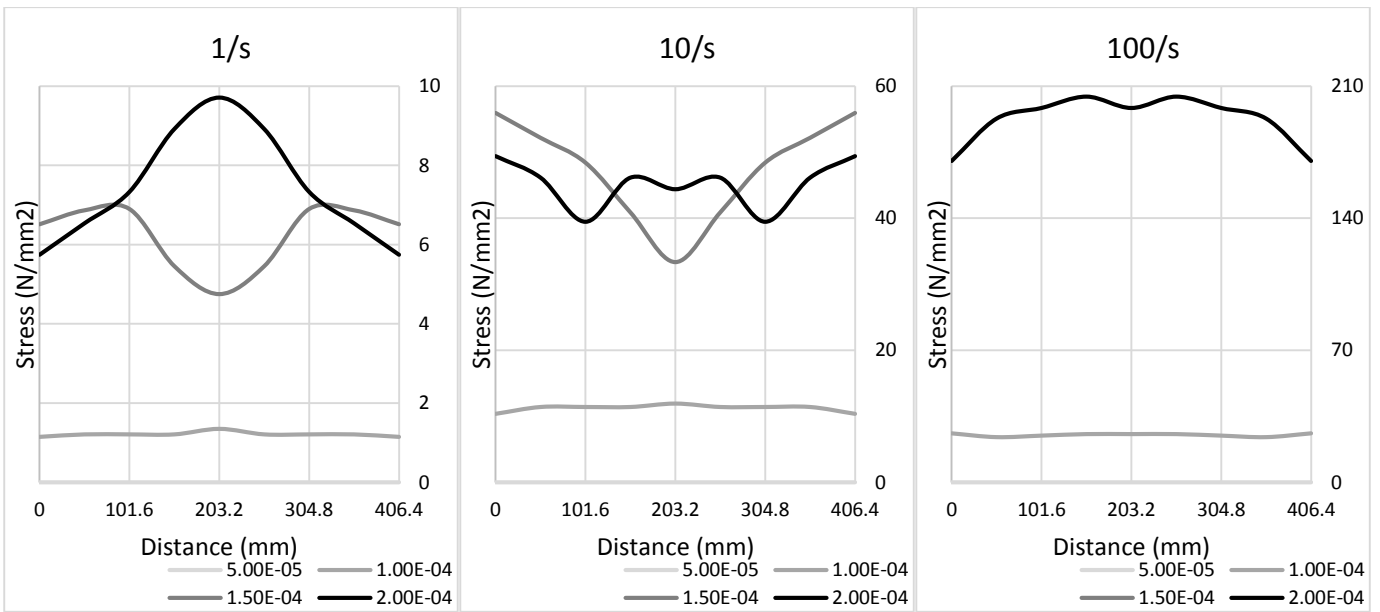


Figure 3-16: Stress history along diameter for 16 × 32 inches 72R3 column at half height for various strain rates at various times.

### 3.7 Summary and Conclusions

From the results of simulation for concrete with a quasi-static compressive strength equal to 46 MPa, the following conclusions can be drawn:

1. For lower strain rates (1/s) the stress wave propagates through the material at lower stress values, seemingly about 3 N/mm<sup>2</sup> for both the material models. The subsequent stress changes are produced by the reflection of the elastic wave and the stress build-up associated with a constant increase in the applied displacement at the loaded end. The ultimate failure is produced at a stress equal to 60 MPa which is higher than the quasi-static compressive strength.
2. For strain rate of 10/s a compression stress wave of magnitude 65 MPa propagates through the material. The initial stress wave is associated with a sharp front and decreasing stress associated with the post-peak material response under increasing strain. There is a decrease in the amplitude of this stress wave amplitude as it propagates in the material due to dissipation produced by material damage. The material however has significant residual strength. The reflected compression stress wave eventually produces failure at 70MPa.
3. For strain rate of 100/s, the stress wave propagates through the material at a stress value of about 90 N/mm<sup>2</sup> for CSCM and about 120 N/mm<sup>2</sup> for 72R3 model. The rate of stress and the stress amplitude produced. The stress wave as it propagates destroys the concrete material, disintegrating it into piece, leaving no chance for reflected waves to come or be observed for strain rates of 100/s.

## CHAPTER 4: Summary and Future Work

The dynamic response of concrete subjected to different strain rates is investigated. The response of various material models in LS Dyna that are commonly used for modelling the dynamic loading on concrete are evaluated for studying the stress response of concrete at different strain rates. The findings of this study are summarized and directions for future research are presented in the next few sections.

### 4.1 Summary

At high strain rates failure is localized. When the strain rate is increased, localized failure is associated with the compressive stress wave generated in the material which produces an abrupt rise in the stress. The initial response is dictated by propagation of the stress wave in the material. The stress changes produced by the propagation of the stress wave are due to linear elastic wave for low strain rates. High strain rates are associated with stress changes produced by a non-linear compression stress wave. The passage of the wave produces irreversible damage and plastic deformation. At very high strain rates, a compression front which produces localized failure is transmitted in the material. The passage of the stress front produces complete crushing failure in the material. As the crushing front propagates in the material, the energy dissipation from the irreversible compaction of the material produces a continuous decrease in the stress amplitude of the compression front.

The magnitude of the stress achieved depends on the rate of loading and the inertial confinement effects. Both effects are important in determining the load response of a reinforced concrete structure. Confinement effects result in an increase in the stress magnitude for a given strain rate. This would result in a stiffening in the load response of the structure. The material strain rate effect results in an increase in the effective strength, which is also compounded by the confinement effect. Locally, significantly higher stresses are produced on increasing the rate of loading and the size of the specimen.



## 4.2 Future work

The directions of future work which emerge from this work are as follows:

1. Evaluating the residual strength of reinforced concrete structural elements subjected to blast pressure loadings of different intensities and durations.
2. Developing Pressure Impulse diagrams in MATLAB for columns subjected to blast loading and their comparison with the LS-DYNA results.
3. Understanding the progressive collapse mechanism, and implementing it in the numerical simulations.

## References

- [1] Bao, X. a. (2010). "Residual Strength of Blast Damaged Reinforced Concrete Columns. *International Journal of Impact Engineering*, 295-308.
- [2] Biggs, J. (1964). *Introduction to Structural Dynamics*. New York: McGraw-Hill.
- [3] Bischoff, P. (1991). Compressive behaviour of concrete at high strain rates. *Materials and Structure*, 425-450.
- [4] Broadhouse, B. N. (October, 1987). *Modelling reinforced concrete structures in DYNA 3D*.
- [5] Clough, R. W. (1993). *Dynamics of Structure*. New York: 2nd edition, McGraw-Hill.
- [6] Dyna, L. (n.d.). *LS Dyna Keyword manual*.
- [7] Dyna, L. (March 2006). *LS-DYNA Theory Manual*. LS Dyna.
- [8] FEMA428. (December 2003). *Design Safe School Projects in Case of Terrorist Attacks*.
- [9] Force, U. A. (1990). *TM 5-1300*.
- [10] Grote, D. P. (2001). Dynamic behaviour of concrete at high strain rates and pressures. *Journal of Impact Engineering*, 869-886.
- [11] Hentz, S. D. (2004). Discrete Element Modelling of Concrete Submitted to Dynamic Loading at High Strain Rates. *Computers & Structures*, 2509-2524.
- [12] Kotsovos, M. D. (1987). Consideration of Triaxial Stress Conditions in Design: a Necessity. *ACI*, 8.
- [13] Krauthammer, T. (1998). Blast Mitigation Technologies: Developments and Numerical Considerations for Behavior Assessment and Design. *International Conference on Structures Under Shock and Impact, Computational Mechanics Inc. SUSI*.
- [14] Li, Q. . (2004). An explanation for rate effect of concrete strength based on fracture toughness including free water viscosity. *Engineering Fracture Mechanics*.
- [15] Li, Q. a. (2002). Pressure-Impulse Diagram for Blast Loads Based on Dimensional Analysis and Single-Degree-of-Freedom Model. *Journal of Engineering Mechanics*, 87.

- [16]Malvar, L. J. (1997). A Plasticity Concrete Material Model for DYNA 3D. *International Journal of Impact Engineering*, 847-873.
- [17]Malvar, L. J. (1998). Review of Static and Dynamic Properties of Steel Reinforcing Bars. *ACI Materials Journal*, 609-616.
- [18]Murray, Y. D. (2007). *Evaluation of LS-DYNA Concrete Material Model 159*. U.S Department of Transportation:.
- [19]Murray, Y. D. (May 2007). *USERS MANUAL FOR LS-DYNA CONCRETE MATERIAL MODEL 159*.
- [20]Ngo, T. M. (2004). High strain rate behaviour of concrete cylinders subjected to uniaxial compressive impact loading. *Proc. of 18th Australasian Conference on the Mechanics of Structures and Materials*. Perth, Australia.
- [21]Ross, C. A. (1995). Effects of Strain Rate on Concrete Strength. *ACI Material Journal*.
- [22]Rossi, P. (1997). Strain Rate Effects in Concrete Structures: the LCPC Experience. *Materials and structures*, 54-62.
- [23]Schuler H, M. C. (2003.). Experimental determination of damage parameter and implementation into a new damage law. *11th international symposium on interaction of the effects of munitions with structures*. Mannheim, Germany.
- [24]Smith, S. J. (2009). *Blast Resistant Design Guide for Reinforced Concrete Structures*. Skokie, Illinois: Portland Cement Association.
- [25]T. Ngo, P. M. (2007). *Blast Loading and Blast Effects on Structures – An Overview*.
- [26]Tedesco, J. W. (1990). Numerical analysis of high strain rate concrete direct tension tests. *Computers and Structures*, 313-327.
- [27]Tedesco, J. W., & Ross, A. C. (1993). Experimental and Numerical Analysis of High Strain Rate Splitting-Tensile Tests. *Materials Journal*, 162-169.
- [28]U.S. ARMY CORPS, N. F. (December, 2008). *UFC 3-340-02*. Department of Defense.
- [29]US Department of the Army, N. a. (1990). The Design of Structures to Resist the Effects of Accidental Explosions. In N. a. US Department of the Army, *TM 5-1300*.
- [30]Williams, G. D. (2009). *Analysis and Response Mechanisms of Blast-Loaded Reinforced Concrete Columns*. Austin, Texas: The University of Texas at Austin.

- [31]Y. Hao, H. H. (2007). Experimental confirmation of some factors influencing dynamic concrete compressive strengths in high-speed impact tests. *Cement and Concrete Research*, (pp. 63 - 70).
- [32]Yong Lu, K. X. (2004). Modelling of dynamic behaviour of concrete materials under blast loading. *International Journal of Solids and Structures*, 131-143.